remote sensing

MDPI

Article

Comparing Three Different Ground Based Laser Scanning Methods for Tree Stem Detection

Ivar Oveland [1,*], Marius Hauglin [2], Francesca Giannetti [3], Narve Schipper Kjørsvik [4] and Terje Gobakken [2]

1 Faculty of Science and Technology, Norwegian University of Life Sciences, 1432 Ås, Norway
2 Faculty of Environmental Sciences and Natural Resource Management, Norwegian University of Life Sciences, 1432 Ås, Norway; marius.hauglin@nmbu.no (M.H.); terje.gobakken@nmbu.no (T.G.)
3 Department of Agricultural, University of Florence, 50145 Firenze, Italy; francesca.giannetti@unifi.it
4 TerraTec AS, 0281 Oslo, Norway; narve.kjorsvik@terratec.no
* Correspondence: ivar.oveland@nmbu.no; Tel.: +47-4022-0711

Received: 4 February 2018; Accepted: 30 March 2018; Published: 31 March 2018

Abstract: A forest inventory is often carried out using airborne laser data combined with ground measured reference data. Traditionally, the ground reference data have been collected manually with a caliper combined with land surveying equipment. During recent years, studies have shown that the caliper can be replaced by equipment and methods that capture the ground reference data more efficiently. In this study, we compare three different ground based laser measurement methods: terrestrial laser scanner, handheld laser scanner and a backpack laser scanner. All methods are compared with traditional measurements. The study area is located in southeastern Norway and divided into seven different locations with different terrain morphological characteristics and tree density. The main tree species are boreal, dominated by Norway spruce and Scots pine. To compare the different methods, we analyze the estimated tree stem diameter, tree position and data capture efficiency. The backpack laser scanning method captures the data in one operation. For this method, the estimated diameter at breast height has the smallest mean differences of 0.1 cm, the smallest root mean square error of 2.2 cm and the highest number of detected trees with 87.5%, compared to the handheld laser scanner method and the terrestrial laser scanning method. We conclude that the backpack laser scanner method has the most efficient data capture and can detect the largest number of trees.

Keywords: backpack laser scanner; forest inventory; handheld laser scanner; lidar; terrestrial laser scanner; tree stem detection

1. Introduction

Updated information about forest resources is important on different scales ranging from the individual tree up to regional, national and global levels. Remote sensing has played a key role in the past decades' development of modern forest inventory methods. Optical sensors on airborne and spaceborne platforms are being used for mapping of forest resources, and, in the boreal forest in the Nordic countries, a majority of operational forest inventories are today carried out using a combination of aerial imagery and data from airborne laser scanning [1]. In this inventory method, the relationship between remotely sensed data and field measured properties is modeled for area units [2]. Complete coverage forest inventory data are produced by utilizing the remotely sensed data and the established relationship with biophysical forest characteristics from the field measurements. A requirement in this approach is that field reference data are available. At a regional and national scale, similar methods have been used with satellite imagery [3]. Field reference data are also required and used in this case.

Manual field registrations including tree positioning, as required in many forest inventory methods, can be time consuming (cf. [4]), and several studies have investigated how remote sensing technologies can aid or replace manual work in the field. Liang et al. [5] reviewed research aiming at using terrestrial laser scanner (TLS) in forest inventories. TLS produces three-dimensional data in the form of dense point clouds, and by processing and analyzing these point clouds several biophysical characteristics related to the forest and the trees can be extracted. Methods have been developed for automatic identification of tree stems and extraction of stem diameters [6–11]. Others have developed methods for more detailed reconstruction of the tree stem and branch structure [12]. It has been suggested that the field reference data that are used in remote sensing based forest inventories can be collected using TLS. Field reference data for forest inventories typically consist of measurements on field plots of size 200–400 m^2. Several challenges must be overcome to effectively use TLS for registrations on field plots, and many of them are discussed in the review studies by Liang et al. [5] and Dassot et al. [13]. Scanning from a fixed position on a field plot will for example lead to occluded areas, or areas where the point cloud data are sparse or missing due to obstructions between the trees and the scanner position. The presence of such occluded areas in the dataset can be reduced by scanning from multiple positions. This is however time consuming, and some studies investigate methods to correct for the missing trees that will be obstructed from the view of the scanner [14]. Reducing the chance of having occluded areas in the data from a field plot can also be achieved by using mobile laser scanning (MLS). Rather than scanning from fixed positions, such systems will continuously record data while the instrument is carried through the forest field plot. The instrument can be carried by a human [8,15,16], or mounted on a vehicle [17,18].

Oveland et al. [8] have developed and described a MLS-based system for acquisition of single tree positions and diameters at forest field plots. This system used data from an airborne laser scanning to determine the ground level. The dependence on additional external data limited the use of the system. It was therefore desirable to develop a system that could be used without the need for additional data. The system described in the current study solves this by including an additional scanning device, and therefore does not depend on additional data. In the following, this system will be referred to as the backpack laser scanner (BPLS). The BPLS system has similar laser instrumentation as the Leica Pegasus backpack tested by Masiero et al. [19].

Previous studies on laser scanner based systems for mapping of trees are briefly described in the following. Pierzchala et al. [20] used an unmanned vehicle-based MLS system and simultaneous localization and mapping (SLAM) to map trees and estimate diameter at breast height (DBH). A root mean square error (RMSE) of 2.4 cm was obtained when estimating the DBH. Based on a novel method for tree stem identification, Heinzel and Huber [21] used TLS to estimate DBH, and obtained an RMSE of 2.9 cm. In a study by Bauwens et al. [15], three systems based on TLS and MLS were compared on trees with DBH > 10 cm. For DBH estimation, an RMSE of 1.1 cm was obtained using the MLS-based system. When using TLS for DBH estimation an RMSE of 3.7 cm was obtained for a single scan and 1.3 cm was reported for multiple scans. For a single TLS scan, 78% of the trees were detected. Forsman et al. [17] used a vehicle-mounted MLS system to estimate DBH. Three-dimensional data were obtained by the combination of a two-dimensional laser scanner and the movement of the vehicle. For the trees within 10 m from the vehicle, an RMSE of 3.7 cm was obtained for the estimation of DBH and with a stem detection accuracy variation from 63% to 78%. Liang et al. [22] demonstrated a BPLS system based on a TLS laser scanner in combination with an inertial measurement unit (IMU) and a global navigation satellite system (GNSS) receiver. A tree stem detection accuracy of 82.6% and an RMSE of 5.1 cm on estimation of DBH were reported in that study. Liang et al. [23] proposed a method using separate processing of multiple TLS scans on a forest field plot. They obtained a stem detection accuracy of 95.3% and an RMSE for the DBH estimation in the range from 0.9 cm to 1.9 cm. Corresponding results for a single scan setup were a detection rate of 73.4% and an RMSE for the DHB in the range from 0.7 cm to 2.4 cm. In a study comparing different TLS scanner setups and detection

algorithms, Pueschel et al. [24] estimated the DBH with an RMSE of 0.7–1.2 cm when using multiple TLS scans. For single TLS scans, the RMSE varied from 1.4 cm to 2.4 cm.

Field plots used in remote sensing based forest inventories are required to be accurately positioned. This is typically achieved in manual field work by using survey-grade GNSS receivers. TLS and MLS instruments which record laser data in a local coordinate system must be related to a global coordinate reference system to be used in the inventory process. The three-dimensional point cloud obtained from the laser instruments are usually rotated and translated from the local coordinate system to a global coordinate reference system using targets. Accurate positioning of targets within forests using GNSS can be challenging, and post-processing is often used [25]. The difficulties are poor sky visibility due to the tree canopy. The trees interrupt the GNSS signals, resulting in poor conditions for GNSS measurements. The movement of a MLS system through the forest means however that favorable conditions for GNSS signals are likely to occur at some locations, where the canopy is less dense or absent. This can be utilized, and in combination with information about the orientations and movements, it can be used to retain the current position in areas with poorer GNSS conditions. Use of IMU in combination with GNSS in forests was applied, e.g., by Kaartinen et al. [26], Forsman et al. [17] and Oveland et al. [8], to handle information about the orientations and movements. In the current study, tightly coupled GNSS-IMU post processing software called TerraPos [27] was used to obtain the position throughout the data collections. Additionally, iterative closest point (ICP) algorithm were used to improve the position accuracy within the plots. TerraPos is a multi-purpose software for aided inertial navigation. In addition to standard ambiguity fixed differential GNSS aiding, a wide range of aiding sources and sensors may be used. Typical aiding examples are wheel-based and visual odometry, magnetometers, slave GNSS antenna, velocity constraints and digital elevation model. TerraPos is usually applied to positioning of planes, ships and cars and not commonly used in an MLS system in the forest.

The aim of the current study was to describe a BPLS system for collection of single tree data on field plots in boreal forest. The target was to obtain DBH and tree position in a global reference frame as efficient as possible. The BPLS system used a novel method to extract the DBH without losing precision due to poor GNSS conditions and to extract the tree position in a global reference frame using a GNSS aided inertial navigation system (INS) in combination with a two-step iterative closest point approach. Data obtained with the BPLS system were compared to similar data from two existing scanning systems, namely the handheld laser scanner (HLS) GeoSlam ZEB1 (GeoSlam, Ruddington Fields Business Park, Ruddington, Nottinghamshire, NG11 6JS, United Kingdom) and the TLS Faro Focus 3D x130 (Faro, 250 Technology Park Lake Mary, FL 32746, USA). Data from all three systems were validated against manual field measurements.

2. Materials and Methods

2.1. Study Area

This study was conducted in a boreal forest in Ås municipality in the southeastern part of Norway (59°40′N 10°46′E, 100 m above sea level). The main tree species in this forest are Norway spruce (*Picea abies* (L.) Karst.) and Scots pine (*Pinus sylvestris* L.). Birch (*Betula pubescens* Ehrh.), larch (*Larix deciduae*) and silver fir (*Abies alba* Mill.) are also present. In total, seven circular plots of 500 m^2 were located in the forest. Two of the plots were located in hilly terrains and five plots were located in flat terrains. The plots were measured with four different measurement methods. The different methods were caliper, TLS, HLS and BPLS. The caliper dataset act as the reference in this study. All other observations were compared to the reference.

2.2. Reference Data Collection

The reference data were collected in May 2017 and October 2017. In total, 335 trees were measured, where 92 trees had a DBH < 10 cm. Table 1 summarizes the number of trees and species. The stem density varied from 380 to 1380 stems/ha with an average of 967 stems/ha.

Table 1. Summary of trees with species and diameter at breast height (DBH).

		DBH (cm)		
Species	**Number of Trees**	**Min**	**Max**	**Mean**
Spruce [1]	144	4.0	60.7	22.3
Pine	137	9.3	43.5	28.2
Silver fir	32	4.1	81.4	9.4
Birch	22	4.1	9.8	6.1

[1] Norway spruce with larch.

For each tree, the DBH was measured with a caliper, and the position of the tree was recorded. There were different stages involved when the data were established. The first step was to register the center of the plot. GNSS registrations are not well suited for dense forest conditions. To establish a high accuracy position for the center point, two additional points were established. The additional points were located in locations where the sky visibility was more suitable for GNSS measurements. The positions of the two known points were obtained with a survey-grade GNSS receiver and the logging of satellite data for more than 30 min. Accurate positions were derived through post processing using GNSS base station data obtained from the Norwegian mapping authorities. An accurate position for the plot center was then found using a SOKKIA SET5 (Sokkia Topcon, 75-1 Hasunuma-cho, Itabashi-ku, Tokyo 174-8580, Japan) total station and the two GNSS measured points. The time consumption for measuring the center point coordinate was approximately 15 min. Finally, tree positions were obtained using the total station and a prism placed in front of the tree center. The prism constant and tree radius were added to the distance measurements. All trees inside the plot with a DBH larger than 4 cm were registered with position, DBH and species. The DBHs were measured once with the caliper in a random heading direction.

The expected standard deviation of the measured tree position was estimated by adding the different error contributors. This was summed up in an error budget shown in Table 2.

Table 2. Error budget for the tree positions. Standard deviations are approximated based on output from the GNSS post processing software, and inspection of the data.

Description	**Standard Deviation (cm)**
GNSS points coordinates	1
Plot center point coordinate	3
Tree center alignment	3
Distance from tree surface to tree center	1

We assumed that the errors were independent and summarized the variance to estimate the standard deviation for the tree positions:

$$\sqrt{1^2 + 3^2 + 3^2 + 1^2} = 4.5 \quad (1)$$

The reference tree positions were estimated to have a standard deviation of 4.5 cm.

2.3. TLS Data Collection

TLS data were collected with a Faro Focus 3D x130 scanner in May 2017. The laser scanner settings were set to give a point density of 70,000 points per m^2 at 5 m distance from the scanner. Bauwens et al. [15] measured the time consumption for a similar TLS and plot and for one single scan the time consumption was 10 min and 75 min for five scans, without positioning the scan in a global coordinate system. To have a comparable time consumption with the other methods in this study, we decided to only use one single scan per plot. A tripod with the laser scanner was placed at the center of each plot. During the reference data collection, the plot center was physically marked and the global coordinates measured. The center point coordinates were used for positioning the scanner in a global coordinate system. The laser scanner had a build-in magnetometer that was used to orient the scanner. The declination at the project location was 1.9° and the meridian convergence was 1.5°. The magnetometer reading was therefore adjusted with +0.4°. The laser point clouds were extracted using Faro Scene version 7.0. The DBH and tree positions were estimated in Computree, version 3.0 [28] using the "onfensamv2" plugin. The following gives a brief outline of the processing step using the "onfesamv2" plugin for each plot: First, the point cloud was classified into ground and vegetation points. The vegetation points were then filtered using two Euclidean filters to remove noise points. A digital terrain model was created using the points classified as ground, and a slice of points between 1.0 m and 1.5 m above the terrain was extracted. From this slice, large clusters of points were identified. The large clusters were then used to segment the point cloud into single tree clouds. From the single tree clouds, the DBH and the center coordinate of each identified tree stem were automatically extracted. The procedure was developed using the SimpleTree plugin in the Computree Software [29]. The main result was a set of positions and DBH for all automatically identified trees and referred to as the TLS tree data.

2.4. HLS Data Collection

The HLS system GeoSlam ZEB1, was used to collect data in May 2017. The system weight was 665 g and had a 15 m outdoor range [30]. It consisted of a laser ranging device mounted on a spring, and the motion created when the operator walked through the forest was an important part of the measurement technique. A comprehensive description of the instrument can be found in Bosse et al. [31], Bauwens et al. [15], Ryding et al. [16] and Giannetti et al. [32].

A star-shaped walking path used by Bauwens et al. [15] was followed to minimize occluded areas. Bauwens et al. [15] reported the HLS data capture time to be 24 min per plot without positioning the scan in a global coordinate system. This time consumption corresponds to our experience. The data capture started and ended in the plot center. The fixed walking path also ensured several loop closures which improved the navigation solution. To ensure an accurate position and orientation in the local frame SLAM was used. The processing was carried out using the Geoslam cloud processing services [15]. The result was one point cloud for each plot.

Three spherical targets were placed within each plot. The positions of these targets were derived using a total station mounted on a tripod at the plot center, with a time consumption of approximately 5 min. The total station was positioned in the same procedure as described in Section 2.2. The accurate position of each of the spherical targets was therefore known. The point cloud obtained from the GeoSLAM processing was rotated and translated from the local coordinate system to a global coordinate system (EUREF89 UTM32N) using the position of the three spherical targets. The targets were automatically detected and the coordinate system assigned using the Align tool in the CloudCompare software [33]. The RMSE values of the registration reported by CloudCompare, were <6 cm for all plots. Tree positions and DBH were derived from the point cloud using the same approach as for the TLS data, described above. The resulting dataset of tree positions and DBH is referred to as the HLS tree data.

2.5. BPLS Data Collection

A BPLS was developed as an extension of the scanner presented in Oveland et al. [8]. The BPLS was an in-house-build. Standard components were assembled in a metal frame and mounted on a backpack. The complete unit is shown in Figure 1. The main hardware improvement from the scanner presented in Oveland et al. [8] was that an additional laser scanner was added and the navigation system was changed. In this version, the navigation system was a combined IMU and dual GNSS board. The unit was called SBG Ellipse 2D (SBG systems, 1 avenue Eiffel, 78,420 Carrières-sur-Seine, France) and received GNSS signals from the Global navigation system (GPS), Globalnaja navigatsionnaja sputnikovaja Sistema (GLONASS) and the Satellite-based Augmentation System (SBAS). A GNSS antenna called PolaNt-X MF (Septentrio, Greenhill Campus, Interleuvenlaan 15i, 3001 Leuven, Belgium) worked as a master antenna. This antenna collected the main GNSS signals. A GNSS reference station operated by the Norwegian University of Life Sciences was used to calculate the initial position of the system. The maximum distance between the reference station and the plots was 800 m. An additional slave GNSS antenna manufactured by Antcom (Antcom Corporation, 367 Van Ness Way, Suite 602, Torrance, California 90501, USA) was a part of the real time heading calculation.

Figure 1. In-house-built backpack laser scanner.

Two laser scanners were mounted on the backpack. Both scanners received time information from the GNSS system. The main scanner collected data horizontally and the secondary scanner collected vertically. The main function of the horizontal scanner was to detect the tree stems, while the vertical scanner's main purpose was to detect the ground. Both scanners had the product name VLP16 (Velodyne LiDAR, 5521 Hellyer Avenue, San Jose, CA 95138, USA) [34]. Each scanner had 16 individual laser beams with an angle separation of two degrees. This gave a Field of view (FOV) of 30°. All 16 beams rotated continuously around the *z*-axis, as shown in Figure 2. This provided in total a FOV of 30° × 360°. The rotation speed used was 10 scan rotations per second and the pulse repetition rate was 300 KHz. All data were stored and exported to ASCII by Veloview version 3.1.1.

The data collection was performed in July 2017 and the data were collected in a star-shaped pattern similar to the HLS. The data capture was carried out by walking across the plot in a straight line through the plot center. This line was defined as a scan line. For the BPLS system, three scan lines were used per plot while the HLS system used four scan lines. With the BPLS scan pattern, the longest possible distance from a random point inside the plot to the scanner was 6.3 m. To be able to detect a tree, it was necessary to create a circle that represented the tree stem. It is necessary to have three measurements on a tree stem to be able to fit a circle to the measurements. From Oveland et al. [8], we have a formula telling that the smallest detectable tree from 6.3 m has a DBH of 4.2 cm. The resulting

dataset of tree positions and DBH is referred to as the BPLS tree data. The startup and initialization of the BPLS system took approximately 10 min and the average data capture time was 6 min per plot.

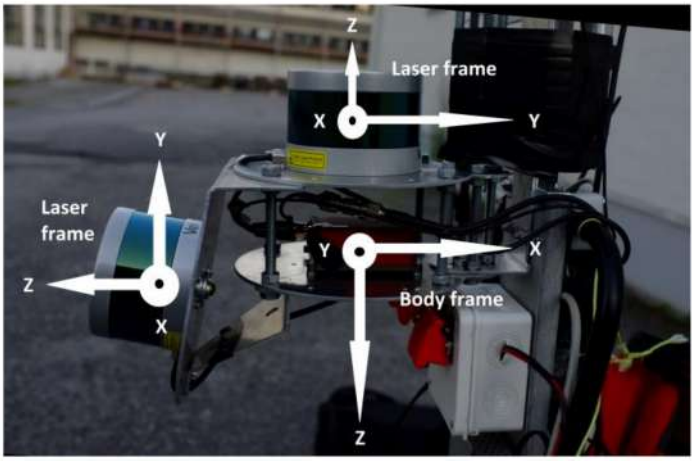

Figure 2. Location and orientation of the vertical and horizontal laser frames and body frame.

BPLS Data Processing

The novel BPLS data processing was divided into nine main steps, as shown in Scheme 1. Steps 2 and 3 are described in more detail by Oveland et al. [8]. In Step 1, position and orientation of the measurement system are calculated. The position and orientation of the measurement system will further be referred to as the pose. In the next steps, the laser data are processed to improve the pose accuracy, and finally calculate the DBH and tree position.

Step 1, illustrated in Scheme 1, was the pose calculation performed in TerraPos version 2.4.90 [27] made by Terratec AS. The input data were raw GNSS data from the main GNSS antenna, 200 Hz IMU data and the heading observation from the combined master and slave GNSS antenna solution. Additional precise ephemeris, clock correction files and earth rotation parameter files were provided from the Center for Orbit Determination in Europe (CODE). The final processing was performed in a tightly coupled GNSS/IMU/heading observation solution. The estimated poses were applied to the laser observations. This was carried out by transforming the measured laser point cloud. There were different reference frames in the BPLS system. The following frames were used:

- laser frame (l), defined by each laser scanner
- body frame (b), defined by the IMU: x-axis: in speed direction; z-axis: down
- local geodetic frame (g), same origo as the body frame: x-axis: north; y-axis: east; z-axis: down
- mapping frame (m), defined by the mapping grid: x-axis: east; y-axis: north; z-axis: up

All laser observations were realized in the laser frame x^{li}, where "i" denoted the vertical or horizontal laser scanner. The laser points in the laser frame were first transformed to body frame x^b. The transformation was performed with the following equation:

$$x^b = C^b_{\widetilde{bi}} C^{\widetilde{bi}}_{li} x^{li} - dx^{li}_b \quad (2)$$

where dx^{li}_b defined the vector from the body frame origo to the specified laser frame origo, measured with a total station. The rotation matrix $C^b_{\widetilde{bi}}$ was used to correct for smaller rotations, also called boresight corrections. $C^{\widetilde{bi}}_{li}$ performed the rough transformation from the laser to the body frame. Figure 2 shows the orientation of the axes for the horizontal laser frame, vertical laser frame and

body frame. The rotation matrix was different for the vertical and horizontal laser scanner and can be written as follows:

$$C_{li}^{\widetilde{bi}}\begin{pmatrix} i = vertical \\ scanner \end{pmatrix} = \begin{bmatrix} 0 & 0 & -1 \\ 1 & 0 & 0 \\ 0 & -1 & 0 \end{bmatrix}, \quad (3)$$

$$C_{li}^{\widetilde{bi}}\begin{pmatrix} i = horizontal \\ scanner \end{pmatrix} = \begin{bmatrix} 0 & 1 & 0 \\ 1 & 0 & 0 \\ 0 & 0 & -1 \end{bmatrix} \quad (4)$$

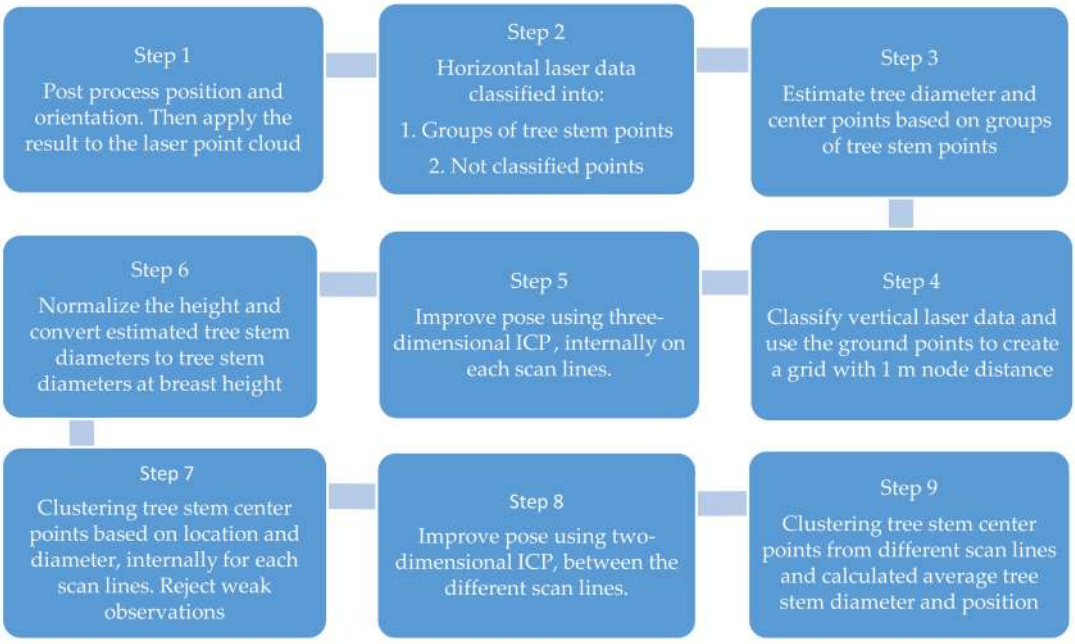

Scheme 1. Flowchart describing each step in the proposed method.

A calibration field was established with two perpendicular lines that were measured in both directions. The field was a parking lot and a road with surrounding buildings, poles and trees. The buildings were additionally measured with a traditional TLS to verify the calibration. The main purpose of the calibration was to estimate the boresight corrections $C_{\widetilde{bi}}^{b}$, and verify the dx_b^{li} vector for each of the scanners. The next transformation was from the body frame to the local geodetic frame x^g. This task was performed using the rotation matrix, C_b^g, created from the orientation estimated in the navigation solution:

$$x^g = C_b^g x^b \quad (5)$$

The last transformation step was from the local geodetic frame to the mapping frame x^m:

$$x^m = C_g^m x^g + dx_g^m \quad (6)$$

The vector dx_g^m was created from the position in the navigation solution. For the BPLS data, the mapping frame was the EUREF89 Norwegian Transversal Mercator projection that has a mapping scale value close to 1 and a small grid conversion. We assumed that the grid conversion was negligible

for this project. The projection gave the rotation matrix C_g^m, transforming from local geodetic to mapping frame:

$$C_g^m = \begin{bmatrix} 0 & 1 & 0 \\ 1 & 0 & 0 \\ 0 & 0 & -1 \end{bmatrix} \quad (7)$$

The pose result had a sampling rate of 200 Hz. It was assumed that the movement during one pose epoch was negligible. Laser points collected in the same time frame as the pose epoch were therefore transformed with the same parameters.

In Step 2, the horizontal laser data were segmented and classified into groups of tree stem points. The method followed the description in Oveland et al. [8].

In Step 3, all groups of tree stem points were used and tree stem diameter and position for each individual group were estimated. It was assumed that the trees were vertical. When four individual point groups were located above each other, they were assumed to be part of the same tree [8].

In Step 4, data from the vertical laser scanner were classified into ground points and non-ground points. After the classification, it was verified that the ground points covered the entire plot and the points were used to establish a grid with node distance of 1 m. These tasks were carried out in TerraScan version 16.004 from Terrasolid [35]. It is assumed that the pose error was relatively stable during one scan line. Between two scan lines, the difference can be significant, especially in height. Thus, for every scan line, a new grid was established. Points classified as ground from different scan lines were not mixed. This reduced the potential influence of deviation in the pose to a minimum.

Due to the poor GNSS condition in the forest, the pose accuracy was reduced compared to a clear sky situation. This made it difficult to merge tree observations based on positions observed at different scan rotations. In Step 5, this problem was reduced by performing scan matching using ICP. Scan matching was divided into two main parts. The first part performed scan matching between sequential scan rotations within a scan line, and the second part performed scan matching between entire scan lines described in Step 8. In both parts, the tree center points were used as input for the scan matching. The estimated tree center points from the first scan rotation at a scan line were used as fixed points. The center point estimation from the next scan rotation was then fitted to the first scan rotation with the ICP algorithm. When the data were fitted, the data were added to the fixed points and so on. One side-effect of this approach was that the entire line inherited the pose accuracy from the first fixed points. This effect was reduced by calculating the average estimated translation from the ICP and applied this to the estimated tree center points.

In Step 6, the established grid from the given scan line was used and the elevation values at the estimated center points were subtracted from the height values. This resulted in tree center positions above ground level. All observations less than 0.5 m above ground were rejected. The goal was to extract the DBH, i.e., 1.3 m above ground level. The estimated diameters were adjusted to diameter at 1.3 m above ground by applying a simple model assuming that the tree diameter was reduced by 1 cm for each meter along the tree stem.

In Step 7, the tree center points were clustered based on position and diameter. We assumed that the diameter was estimated with a standard deviation below 5 cm. If there were two groups within the search radius and the groups had a diameter difference above 15 cm, they were given a different tree identification. The circle points within a scan rotation were analyzed using random sample consensus. This technique was used to reject observations. Tree stem circle points which did not fit in a straight line were rejected. Additional identified trees with five or fewer circle observations per scan line were also rejected.

Step 8 ensured that the result from the different scan lines fitted each other. This was performed with a two-dimensional ICP method between the clustered tree stem center points from the different scan lines.

In Step 9, the results from the different scan lines were merged based on location. Finally, the average position and DBH were derived and compared to the reference.

2.6. Evaluation

The resulting tree positions and DBHs from the TLS, HLS and BPLS tree datasets were compared to the reference data. The estimated DBH were evaluated by calculating the mean difference, RMSE and RMSE% with the following equations:

$$\text{mean difference} = \frac{1}{n}\sum_{i=1}^{n}(y_i - y_{ri}) \tag{8}$$

$$\text{RMSE} = \sqrt{\frac{\sum_{i=1}^{n}(y_i - y_{ri})^2}{n}} \tag{9}$$

and

$$\text{RMSE\%} = \frac{\text{RMSE}}{\overline{y_r}}\,100 \tag{10}$$

In the equations, y_i is the estimate, y_{ri} the reference, $\overline{y_r}$ is the mean reference value, and n the number of observations. The reference was the result from the calipered DBH and manual tree position registrations using total station as described above. The tree position accuracy was evaluated using Equations (8) and (9).

3. Results

The TLS had a built-in magnetometer that was used to orient the scanner. The magnetometer readings were evaluated by rotating the laser scanner result until a best possible fit to the reference tree positions was achieved. Table 3 summarizes the result.

The average heading error was -0.8° with a 6.1° standard deviation. Additionally, the tree positions were calculated based on the magnetometer readings and with the corrections found in Table 3. The result is presented in Table 4.

The evaluation of the magnetometer accuracy showed that the tree position can be significantly better by improving the orientation method. The final result based on the magnetometer readings are presented in Table 5. The DBH estimation for the TLS method had two major outliers. By removing these two outliers, the mean difference was 1.5 cm, the RMSE 3.4 cm and the RMSE% 15.5.

Table 3. The heading error in the magnetometer readings, found by comparing the estimated tree positions from the terrestrial laser scanner method and the tree position from the reference.

Plot ID	Angle Difference in Heading (Degrees)
1	2.0°
2	−9.0°
3	4.9°
4	7.4°
5	1.1°
6	−6.5°
7	−5.2°

Table 4. The result from comparing the archived tree position accuracy with two different orientation methods.

Orientation Method	Mean Difference (cm)	RMSE (cm)
Magnetometer	69.1	81.8
Reference tree position	8.5	9.9

The results obtained from the HLS revealed that small trees were difficult to detect. To illustrate this, one of the plot with a high number of small trees was used as an example. In Figure 3a, the HLS

tree data are plotted in green together with the reference trees in red. Figure 3b shows the laser point in the region 1.0 m to 1.5 m above ground level. By comparing Figure 3a,b, it seems that the missing trees occurred where there were no half or full donut shaped pattern in the laser data.

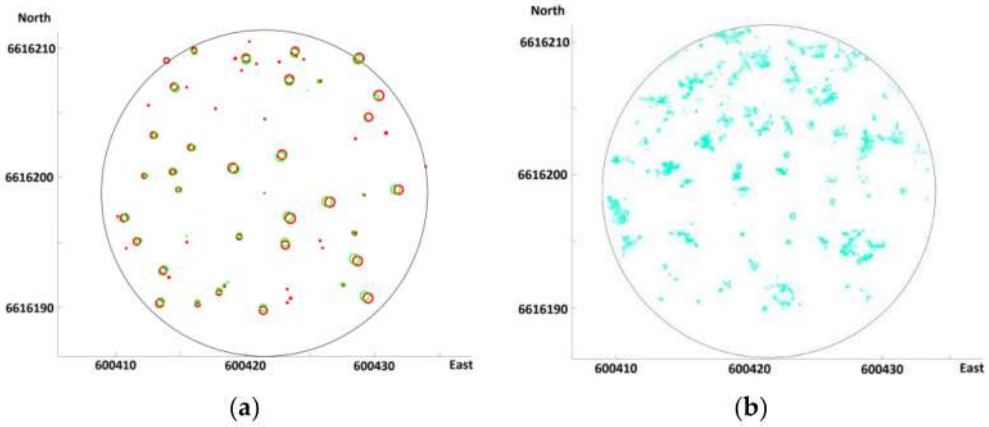

Figure 3. (**a**) Detected trees by HLS (green circle) and ground reference tree data (red circles). The size of the circle represents the DBH and the coordinate system is EUREF89 UTM zone 32. (**b**) HLS data used to extract trees.

An important factor for the BPLS method was the calculated pose accuracy. The estimated standard deviation for the position was better than 0.5 m. For roll and pitch it was better than 0.13° and for heading it was better than 0.9°. The combined master and slave GNSS antenna heading system had only 134 epochs with valid observations. The heading system was very useful during system orientation initialization. Inside the forest the position dilution of precision (PDOP) varied from 1.1 to 17. Typically, TerraPos was able to create fixed solutions when the PDOP dropped down and float solutions when it rose. Approximately 60% of the epochs had a fixed solution, but in the densest forest there were up to 18 min in-between two fixed solutions. Due to the tightly coupled solution, there were continually pose observations for the entire mission. The main result from the different methods is presented in Table 5.

The results presented in Table 5 show that up to 37.9% of the trees were not found. Table 6 presents the average DBH for the omission trees and the number of trees with DBH larger and smaller than 10 cm.

Table 5. Comparison of the results derived from the terrestrial laser scanner (TLS), handheld laser scanner (HLS) and the backpack laser scanner (BPLS). The total number of trees were 335.

Method	Omission (Not Found) %	Commission (False Trees) %	Detected Trees %	Diameter at Breast Height (cm)			Positions (cm)	
				Mean Difference	RMSE	RMSE %	Mean Difference	RMSE
TLS	37.9	5.4	61.8	-2.0	6.2	28.6	69	82
HLS	26.0	4.8	74.0	0.3	3.1	14.3	17	20
BPLS	12.5	9.9	87.5	0.1	2.2	9.1	54	62

Table 6. The average diameter at breast height (DBH) for omission trees.

Method	Average DBH for Omission Trees (cm)	Number of Omission Trees with DBH < 10 cm	Number of Omission Trees with DBH > 10 cm
Terrestrial laser scanner	16.9	67	60
Handheld laser scanner	8.7	68	19
Backpack laser scanner	7.5	36	6

4. Discussion

The coordinate for the plot center point was determined using GNSS measurements in relatively clear sky locations and measured using a total station. These established center points were also used to position the HLS and TLS data. This gave a correlation between these measurement methods and the reference data while the BPLS data were independent. Thus, the resulting uncertainties in the center point coordinates would not affect the HLS or TLS data positions statistics but would give a false position offset for the BPLS result. We assume that there were no major errors in the center point position estimation and that the errors were independent of each other. The errors presented in Table 2 are summarized:

$$\sqrt{st.dev\ GNSS\ measurment^2 + st.dev\ plot\ center\ point\ measurment^2} = \sqrt{1^2 + 3^2} = 3.2\ \text{cm} \quad (11)$$

The center point coordinates were estimated to have a standard deviation of 3.2 cm. This was substantially less than the achieved standard deviation for all the laser scanning methods.

The caliper measurements of the DBH were conducted with one measurement in a random heading direction. Since tree stems can be ellipse-shaped, DBH measured from a different direction might deviate from this reference measurement. This can be viewed as a small uncertainty in the reference measurements, and might have an influence on the achieved DBH accuracy. The uncertainties could have been reduced by using an additional perpendicular caliper measurement or using diameter tape to measure the girth.

As shown in Figure 3a, the HLS had difficulties to detect smaller trees and this confirmed the results underlined by Bauwens et al. [15] and Ryding et al. [16]. In the situation where the HLS data formed a half or full donut shape pattern, the tree detection technique worked well (Figure 3b). Other shapes such as filled circle and odd shapes did not succeed at the same level. One reason for the blurry shapes describing the smaller trees might be the point cloud precision. Another reason might be a change in the stem inclination due to wind conditions [21]. All laser scanners had problems to detect the smaller trees. Additionally, the TLS had problems with occluded areas, since the scanning was performed only from the center. The average tree density in our study area was 969 stems/ha, but also the high number of small trees that created a complex understory vegetation contributed to the occluded areas. Both the HLS and BPLS were carried around in the plot. This reduced the occluded areas to a minimum, but there will always be some occluded areas left due to branches, leaves and bushes. The BPLS method found the largest number of trees, also when it comes to the smallest trees.

For the BPLS method, it was important to capture all the potential GNSS satellites in the forest. This was important to ensure the best possible position in the global coordinate frame. The GNSS equipment used in the BPLS could not receive signals from the GNSS created by the European Union called Galileo. The base station was able to pick up some signals from the Chinese BeiDou navigation satellite system, but these signals were not present in the BPLS GNSS data. BeiDou and Galileo together consist of 15–20 satellites. Under good GNSS observation conditions, it might have been possible to track 7–10 more satellites. Inside the forest, this could give a huge difference because just one more observed satellite could create a fix solution rather than a float solution. Signals from both Galileo and BeiDou could have improved the position accuracy. The DBH calculation for the BPLS was not vulnerable to poor GNSS condition, but the processing was smoother if the position standard deviation was below 0.5 m. The main reason for the low sensitivity to poor GNSS was the INS and the splitting of the laser data. The proposed method splits the laser data into small time frames, decided by the scan rotation of the horizontal VLP 16 laser scanner. For each 0.1 s, a new point cloud was established. This point cloud was then used to estimate the tree center point and stem diameter. ICP operations were applied to the result and ensured a homogenous localization of each tree with the corresponding attributes. This method ensured that errors from GNSS and IMU are negligible to the stem diameter and DBH calculation. This assumption was acceptable since the pose error can be considered as stable within such time interval. A side effect was the high number of point clouds, where each of them gave

diameter calculation for the observed trees. The result was many diameter calculations that were used to estimate the final DBH for each tree. This had a positive impact on the DBH accuracy.

Each method used different workflows with different working tasks involved. The data capture time would mainly vary according to the number of tasks. The most time consuming method was the HLS method. This technique required static GNSS, position of the plot center, spheres position measurements and laser scanning. The total time consumption was estimated as 74 min. Some of the working tasks can be done in parallel to reduce the time consumption. However, this was not considered in this study. Table 7 summarizes the time consumption from this and previous studies. The overview shows that the BPLS was the method with the fewest working tasks, and therefore, the fastest method with an estimated time consumption of 16 min.

Table 7. The different working tasks and time consumption per plot for each laser based method.

Method	Static GNSS for Reference Points	Position Measurement of Plot Center	Position Measurement of Spheres	Laser Scanning	Total
Terrestrial laser scanner	30 min	15 min		10 min	55 min
Handheld laser scanner	30 min	15 min	5 min	24 min	74 min
Backpack laser scanner				16 min	16 min

The TLS was aligned with a built-in magnetometer. The precision of the final tree coordinates was heavily influenced by the quality of the built-in magnetometer. If the registration of the center point positions was carried out using a total station, it would not be very time consuming to put up spheres to align the scanner and thus obtain a much better precision. On the other hand, the TLS data were very homogenous in the sense that the relative positions within each plot were consistent. Thus, the highly accurate tree positions of the detected trees are a really good starting point as input for matching the data with airborne laser data [36], to improve position accuracy.

The main data capture was performed in May 2017, before the leaves had emerged. The BPLS data collection was delayed due to technical problems and was performed in early July 2017. The leaves had emerged, which might have had an effect on the tree stem visibility and the number of false trees. An example from plot number three is shown in Figure 4a,b. The tree growth between the two points in time were assumed to have a minor effect on the DBH.

The data capture with the BPLS was carried out by walking across each plot in straight lines forming a star-shaped pattern. The number of lines decided the maximum possible distance to the potential trees inside the plot. In this study, we used three scan lines and this gave a theoretical minimum detectable DBH of 4.2 cm for the BPLS. In the reference data, the minimum DBH was set to 4.0 cm. This means that there are small areas at the outer edge where we were unable to detect the smallest trees. In this study, the total area was 0.4% of a plot and was assumed to be at an acceptable level.

For a long time, studies have reported large commission errors [37] when laser based methods have been used. More recent studies confirm these observations [15,22]. Reported commission errors vary from 0% to 31% [15]. The result in our study showed that the number of false trees—i.e., commission errors—were up to 9.9% of the total number of field reference trees. Most of the false trees had a DBH less than 10 cm. In the reference data, all trees with a DBH larger than 4 cm were measured. No trees with a smaller DBH than 4 cm were measured. Since the measurement methods have uncertainties, it is possible that some of the trees which were estimated to have a larger DBH than 4 cm actually were trees with DBH smaller than 4 cm. In such situations, the trees would be registered as false trees. In the BPLS method, the laser point clouds were segmented into tree points, ground points and none classified points. The segmentation was based on a rule based approach. This could in further studies be changed to a machine learning approach. This has the potential to improve the tree segmentation and reduce the commission errors.

Figure 4. (**a**) Understory vegetation in May 2017. (**b**) Understory vegetation in July 2017 at the same location as (**a**).

The obtained results for the DBH estimation are compared to results in other recent studies in Table 8. All TLS methods in Table 8 were performed with one single scan in the center of the plot. Our TLS result had a lower accuracy compared to similar studies [15,23,24]. Potential explanations for this might be the tree density and the understory vegetation and how this affect the DBH calculation. Other elements that might affect the DBH extraction are the ranging method in the laser scanner, the scanner characteristics, scan settings and data processing [24]. The TLS method in our study had two large outliers. An outlier search might have detected these outliers and thus reduced the RMSE and RMSE% to 3.4 cm and 15.5, respectively.

Table 8. Comparison of current results with previous studies derived from the terrestrial laser scanner (TLS), handheld laser scanner (HLS) and the backpack laser scanner (BPLS). * mean value calculated from Liang and Hyyppä [23]. ** single scan, Lemen algorithm, beech plot [24].

Reference	Method	Equipment	Mean Difference (cm)	RMSE (cm)	RMSE%
This study	TLS	Faro Focus 3D x130	−2.0	6.2	28.6
[15]	TLS	Faro Focus 3D x120	−1.2	3.7	13.4
[23]	TLS	Leica HDS6100	0.5*	1.5*	7.3*
[24]	TLS	Faro photon 120	−0.1**	1.6**	-
This study	HLS	GeoSlam ZEB1	0.3	3.1	14.3
[15]	HLS	GeoSlam ZEB1	−0.1	1.1	4.1
[16]	HLS	GeoSlam ZEB1	0.5	2.9	23
This study	BPLS	Velodyne VLP 16	0.1	2.2	9.1
[8]	BPLS	Velodyne VLP 16	0.9	1.5	7.5

In general, the TLS, HLS and BPLS result in this study have larger RMSE and RMSE% values compared to other studies. One advantage of our study was that the different methods have the same preconditions regarding stem density, tree species, stem sizes, understory vegetation, reference data and plot size. This makes it easier to compare the different methods used in the study. On the other hand, the DBH extraction algorithm for the TLS and HLS method might vary from the state-of-the-art DBH. In this study, the BPLS method achieved the best accuracy with the smallest level of omissions, however the largest level of commissions was also obtained.

BPLS seems to be a very promising method in terms of time consumption for data collection. Thus, BPLS might have great potential as a cost-effective data source in forest inventory. Moreover, a final decision about the most profitable source of data for forest inventory should not be based on purely technical considerations, such as reported accuracies. It is of fundamental importance for management that the costs of acquiring the information are balanced against the utility of the information for decision-making. Thus, we recommend that future research focus on this trade-off using for example so-called cost-plus-loss analyses, which may establish a link between errors

associated with the inventory and expected losses as a result of future incorrect decisions due to the errors in the data.

5. Conclusions

In this study, we have proposed a novel laser based BPLS method for acquisition of ground references data and compared the method with other laser based systems. The proposed method is a further development of the method presented in Oveland et al. [8]. Novel aspects in the method are how the trees are segmented and how the diameters at breast height are estimated without losing precision due to potential reduced position and orientation accuracy. Most importantly, the trees are directly positioned in a global coordinate system using a GNSS aided inertial navigation system in combination with an iterative closest point approach. The study has compared three different laser based methods to extract the diameter at breast height and tree position within seven different plots. The different methods are BPLS, HLS and TLS. Comparison with manual measurements shows that the TLS method in general had the most consistent positioning of the trees, but is vulnerable to occluded areas. The HLS method has difficulties detecting smaller trees. The fastest and most accurate method in this study is the BPLS, where the diameter at breast height has a mean difference of 0.1 cm, root mean square error of 2.2 cm and the largest amount of detected trees with 87.5%. The BPLS has however the highest number of false trees and the tree positions are slightly degraded, but the position accuracy should be acceptable for many forestry inventory purposes. Thus, the BPLS seems to be promising and further development should be focused on the possibility to go from a GNSS aided inertial navigation system to a GNSS and laser odometry aided inertial navigation system in combination with simultaneous localization and mapping. Cost-plus-loss analyses of the final forest inventory results assessing required accuracy of ground reference data should also be subject to further research.

Supplementary Materials: The following are available online at http://www.mdpi.com/2072-4292/10/4/538/s1, Video 20170703_backpack_scanner.mp4: Data collection with the backpack laser scanner system.

Acknowledgments: The study was partly funded by the Research Council of Norway through the project "Sustainable Utilization of Forest Resources in Norway" (grant #225329/E40).

Author Contributions: Ivar Oveland wrote the paper, performed the BPLS fieldwork, conducted the hardware installation, method development, and processed the data. Marius Hauglin co-authored the paper, performed the TLS fieldwork, the caliper fieldwork and processed the data. Francesca Giannetti performed the HLS fieldwork and processed the data, performed the caliper fieldwork and revised the paper. Narve Schipper Kjørsvik provided the GNSS/IMU processing tool, supported the pose processing and revised the paper. Terje Gobakken supervised the study and revised the paper.

Conflicts of Interest: Narve Schipper Kjørsvik works at Terratec AS which is a GNSS/IMU software dealer. The authors declare no conflict of interest.

References

1. Vauhkonen, J.; Maltamo, M.; McRoberts, R.E.; Næsset, E. Introduction to forestry applications of airborne laser scanning. In *Forestry Applications of Airborne Laser Scanning*; Springer: Berlin, Germany, 2014; pp. 1–16.
2. Næsset, E. Practical large-scale forest stand inventory using a small-footprint airborne scanning laser. *Scand. J. For. Res.* **2004**, *19*, 164–179. [CrossRef]
3. Gjertsen, A.K. Accuracy of forest mapping based on Landsat TM data and a kNN-based method. *Remote Sens. Environ.* **2007**, *110*, 420–430. [CrossRef]
4. Breidenbach, J.; Næsset, E.; Lien, V.; Gobakken, T.; Solberg, S. Prediction of species specific forest inventory attributes using a nonparametric semi-individual tree crown approach based on fused airborne laser scanning and multispectral data. *Remote Sens. Environ.* **2010**, *114*, 911–924. [CrossRef]
5. Liang, X.; Kankare, V.; Hyyppä, J.; Wang, Y.; Kukko, A.; Haggrén, H.; Yu, X.; Kaartinen, H.; Jaakkola, A.; Guan, F.; et al. Terrestrial laser scanning in forest inventories. *ISPRS J. Photogramm. Remote Sens.* **2016**, *115*, 63–77. [CrossRef]

6. Liang, X.; Litkey, P.; Hyyppa, J.; Kaartinen, H.; Vastaranta, M.; Holopainen, M. Automatic Stem Mapping Using Single-Scan Terrestrial Laser Scanning. *IEEE Trans. Geosci. Remote Sens.* **2012**, *50*, 661–670. [CrossRef]
7. Lindberg, E.; Holmgren, J.; Olofsson, K.; Olsson, H. Estimation of stem attributes using a combination of terrestrial and airborne laser scanning. *Eur. J. For. Res.* **2012**, *131*, 1917–1931. [CrossRef]
8. Oveland, I.; Hauglin, M.; Gobakken, T.; Næsset, E.; Maalen-Johansen, I. Automatic Estimation of Tree Position and Stem Diameter Using a Moving Terrestrial Laser Scanner. *Remote Sens.* **2017**, *9*, 350. [CrossRef]
9. Simonse, M.; Aschoff, T.; Spiecker, H.; Thies, M. Automatic Determination of Forest Inventory Parameters Using Terrestrial Laserscanning. Available online: http://www.natscan.uni-freiburg.de/suite/pdf/030916_1642_1.pdf (accessed on 30 March 2018).
10. Strahler, A.H.; Jupp, D.L.B.; Woodcock, C.E.; Schaaf, C.B.; Yao, T.; Zhao, F.; Yang, X.; Lovell, J.; Culvenor, D.; Newnham, G.; et al. Retrieval of forest structural parameters using a ground-based lidar instrument. *Can. J. Remote Sens.* **2008**, *34*, S426–S440. [CrossRef]
11. Yao, T.; Yang, X.; Zhao, F.; Wang, Z.; Zhang, Q.; Jupp, D.; Lovell, J.; Culvenor, D.; Newnham, G.; Ni-Meister, W.; et al. Measuring forest structure and biomass in New England forest stands using Echidna ground-based lidar. *Remote Sens. Environ.* **2011**, *115*, 2965–2974. [CrossRef]
12. Raumonen, P.; Kaasalainen, M.; Åkerblom, M.; Kaasalainen, S.; Kaartinen, H.; Vastaranta, M.; Holopainen, M.; Disney, M.; Lewis, P. Fast Automatic Precision Tree Models from Terrestrial Laser Scanner Data. *Remote Sens.* **2013**, *5*, 491–520. [CrossRef]
13. Dassot, M.; Constant, T.; Fournier, M. The use of terrestrial LiDAR technology in forest science: Application fields, benefits and challenges. *Ann. For. Sci.* **2011**, *68*, 959–974. [CrossRef]
14. Astrup, R.; Ducey, M.J.; Granhus, A.; Ritter, T.; von Lüpke, N. Approaches for estimating stand-level volume using terrestrial laser scanning in a single-scan mode. *Can. J. For. Res.* **2014**, *44*, 666–676. [CrossRef]
15. Bauwens, S.; Bartholomeus, H.; Calders, K.; Lejeune, P. Forest Inventory with Terrestrial LiDAR: A Comparison of Static and Hand-Held Mobile Laser Scanning. *Forests* **2016**, *7*, 127. [CrossRef]
16. Ryding, J.; Williams, E.; Smith, M.; Eichhorn, M. Assessing Handheld Mobile Laser Scanners for Forest Surveys. *Remote Sens.* **2015**, *7*, 1095–1111. [CrossRef]
17. Forsman, M.; Holmgren, J.; Olofsson, K. Tree Stem Diameter Estimation from Mobile Laser Scanning Using Line-Wise Intensity-Based Clustering. *Forests* **2016**, *7*, 206. [CrossRef]
18. Palleja, T.; Tresanchez, M.; Teixido, M.; Sanz, R.; Rosell, J.; Palacin, J. Sensitivity of tree volume measurement to trajectory errors from a terrestrial LIDAR scanner. *Agric. For. Meteorol.* **2010**, *150*, 1420–1427. [CrossRef]
19. Masiero, A.; Fissore, F.; Guarnieri, A.; Piragnolo, M.; Vettore, A. Comparison of low cost photogrammetric survey with TLS and Leica Pegasus Backpack 3D models. *Int. Arch. Photogramm. Remote Sens. Spat. Inf. Sci.* **2017**, *42*.
20. Pierzchała, M.; Giguère, P.; Astrup, R. Mapping forests using an unmanned ground vehicle with 3D LiDAR and graph-SLAM. *Comput. Electron. Agric.* **2018**, *145*, 217–225. [CrossRef]
21. Heinzel, J.; Huber, M.O. Tree Stem Diameter Estimation From Volumetric TLS Image Data. *Remote Sens.* **2017**, *9*, 614. [CrossRef]
22. Liang, X.; Kukko, A.; Kaartinen, H.; Hyyppä, J.; Yu, X.; Jaakkola, A.; Wang, Y. Possibilities of a Personal Laser Scanning System for Forest Mapping and Ecosystem Services. *Sensors* **2014**, *14*, 1228–1248. [CrossRef] [PubMed]
23. Liang, X.; Hyyppä, J. Automatic Stem Mapping by Merging Several Terrestrial Laser Scans at the Feature and Decision Levels. *Sensors* **2013**, *13*, 1614. [CrossRef] [PubMed]
24. Pueschel, P.; Newnham, G.; Rock, G.; Udelhoven, T.; Werner, W.; Hill, J. The influence of scan mode and circle fitting on tree stem detection, stem diameter and volume extraction from terrestrial laser scans. *ISPRS J. Photogramm. Remote Sens.* **2013**, *77*, 44–56. [CrossRef]
25. Andersen, H.-E.; Clarkin, T.; Winterberger, K.; Strunk, J. An accuracy assessment of positions obtained using survey-and recreational-grade global positioning system receivers across a range of forest conditions within the Tanana Valley of interior Alaska. *West. J. Appl. For.* **2009**, *24*, 128–136.
26. Kaartinen, H.; Hyyppä, J.; Vastaranta, M.; Kukko, A.; Jaakkola, A.; Yu, X.; Pyörälä, J.; Liang, X.; Liu, J.; Wang, Y.; et al. Accuracy of Kinematic Positioning Using Global Satellite Navigation Systems under Forest Canopies. *Forests* **2015**, *6*, 3218–3236. [CrossRef]
27. *TerraPos version 2.4.90*; GNSS/INS post processing software; Terratec: Oslo, Norway; Available online: https://www.terratec.no/terrapos (accessed on 16 November 2017).

28. Office National des Forêts. *Computree version 3.0*; A software platform for processing Terrestrial LiDAR data to extract forest information; Office National des Forêts: Paris, France, 2010; Available online: http://computree.onf.fr/?lang=en (accessed on 16 November 2017).
29. Hackenberg, J.; Spiecker, H.; Calders, K.; Disney, M.; Raumonen, P. SimpleTree —An Efficient Open Source Tool to Build Tree Models from TLS Clouds. *Forests* **2015**, *6*, 4245. [CrossRef]
30. Geoslam. *GeoSlam Zeb-1*; Geoslam: Ruddington, Nottinghamshire, UK; Available online: https://geoslam.com/hardware/zeb-1/ (accessed on 16 November 2017).
31. Bosse, M.; Zlot, R.; Flick, P. Zebedee: Design of a spring-mounted 3-d range sensor with application to mobile mapping. *IEEE Trans. Robot.* **2012**, *28*, 1104–1119. [CrossRef]
32. Giannetti, F.; Chirici, G.; Travaglini, D.; Bottalico, F.; Marchi, E.; Cambi, M. Assessment of Soil Disturbance Caused by Forest Operations by Means of Portable Laser Scanner and Soil Physical Parameters. *Soil Sci. Soc. Am. J.* **2017**, *81*, 1577–1585. [CrossRef]
33. Girardeau-Montaut, D. *CloudCompare version 2.8*; Open source 3D point cloud processing software. Available online: http://www.danielgm.net/cc/ (accessed on 16 November 2017).
34. Velodyne Lidar, PUCK, VLP16. Available online: http://velodynelidar.com/vlp-16.html (accessed on 1 October 2017).
35. Anon. *TerraScan User's Guide*; Terrasolid Ltd.: Helsinki, Finland, 2011.
36. Hauglin, M.; Lien, V.; Næsset, E.; Gobakken, T. Geo-referencing forest field plots by co-registration of terrestrial and airborne laser scanning data. *Int. J. Remote Sens.* **2014**, *35*, 3135–3149. [CrossRef]
37. Bienert, A.; Scheller, S.; Keane, E.; Mohan, F.; Nugent, C. Tree Detection and Diameter Estimations by Analysis of Forest Terrestrial Laser Scanner Point Clouds. In Proceedings of the ISPRS Workshop on Laser Scanning 2007 and SilviLaser 2007, Espoo, Finland, 12–14 September 2007; pp. 50–55.